FEATURES OF DENSE PLASMA FORMATION IN THE REFLEX DISCHARGE ON GAS-METAL MIXES

Yu.V. Kovtun
National Science Center "Kharkov Institute of Physics and Technology", Kharkov, Ukraine
E-mail: Ykovtun@kipt.kharkov.ua

The paper briefly summarizes the data from studies of multicomponent gas-metal plasma in a pulsed reflex discharge. The processes of injection of sputtered-and-ionized working materials (Ti, Mo, W, U) into the reflex discharge plasma have been considered in the framework of the steady-state model. The measured data on the rotational velocity of the gas-metal multicomponent plasma formed in the reflex discharge correlate with the critical ionization velocity (CIV) values.

PACS: 52.80.Sm; 68.49. Sf

INTRODUCTION

The plasma in crossed $\boldsymbol{E} \times \boldsymbol{B}$ fields is of interest for solving a wide range of scientific and applied problems in plasma physics, in particular, in the area of research on laboratory, fusion and space plasmas [1]. One of these problems is the study of a highly-ionized dense ($N_e \sim 10^{14}$ cm^{-3}) rotating ($v_\varphi \sim 10$ km/s) plasma and the development of devices for material separation into mass groups and elements [2]. The efficiency of separating devices depends on the solution of two problems: i) injection efficiencies of substances to be separated in plasma; ii) the efficiency of radial ion separation directly depends on the rotational velocity.

The problem of introducing a working material, i.e., the substance to be separated, into the workspace of a magnetoplasma separator can be solved on the basis of the reflex discharge [3] or the discharge of any other type. It is known from the literature [4 - 7] that there are a number of approaches, which can be used for these purposes. Here, the preference is given to the working substance introduction scheme (device), where the reflex discharge is applied.

The reflex discharge-based device for elemental separation of substances has been proposed in [3]. The specific features of the device are as follows: (1) the cathodes either fully consist of a substance to be separated or contain it; (2) plasma formation proceeds in two stages (in the first stage, a foreplasma is produced by ionizing the igniter gas, while in the second stage, the main plasma is formed from the working substance); (3) the cathode surfaces facing the igniting discharge are bombarded by particle fluxes from the foreplasma, due to which sputtered particles of the cathode material (the substance to be separated) are supplied into the discharge.

The previous experience [8 - 12] attests that the reflex discharge is an efficient instrument for producing a multicomponent gas-metal plasma. In this case, the metal plasma component is formed as a result of ionization of cathode material particles that penetrate into the discharge as the material is sputtered.

The present work is a continuation of previous investigations of multicomponent gas-metal plasma in the pulsed reflex discharge [8 - 17]. Here the previously obtained findings are summarized in short. This work has been aimed at analyzing the processes of material injection (due to sputtering) and ionization in a dense gas-metal plasma in the reflex discharge. Consideration was also given to variations of the rotational velocity of the gas-metal multicomponent plasma.

1. EXPERIMENTAL SETUP

The experiments were performed in the gas-metal multicomponent plasma of a pulsed reflex-discharge device MAKET (Fig. 1). The stainless steel discharge chamber had the following dimensions: 20 cm in internal diameter, and 200 cm in length.

The plasma was produced by discharging a capacitor bank between cold cathodes and the anode (the wall of the vacuum chamber). The gas-metal plasma was produced in the mixture of the igniter gas and the sputtered cathode material. Typical operating characteristics for the device MAKET are listed in Table 1.

To study the gas-metal plasma parameters in the pulsed reflex discharge with $N_e = 10^{12}…10^{14}$ cm^{-3}, a variety of diagnostic techniques were used: 1) microwave interferometry at the wavelengths $\lambda = 2.14…11.5$ mm ($N_c = 2.4\cdot10^{14}…8.4\cdot10^{12}$ cm^{-3}); 2) microwave reflectometry at the same wavelengths provided that $N_e \geq N_c$; 3) two-frequency microwave correlation reflectometry for determination of the plasma rotation velocity, 4) optical spectrometry in the wavelength range $\lambda = 220…680$ nm; 5) the time dependence of plasma radiation intensity in the range of wavelengths $\lambda = 180…1100$ nm was measured by a photodiode FDUK-13U; 6) Langmuir probes, and 7) Rogowski loop. The indicated diagnostic means, except for the Rogowski loop, were placed in diagnostic ports, which were located in two cross sections of the vacuum chamber, as illustrated in Fig. 1.

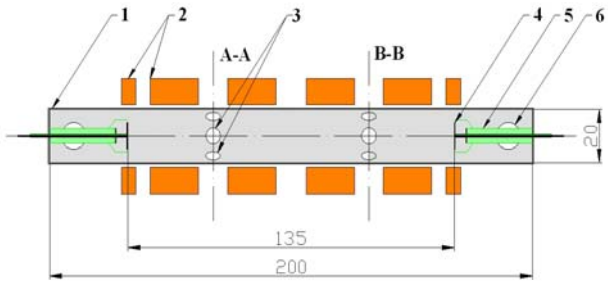

Fig. 1. A schematic drawing of the MAKET device. 1 – vacuum chamber; 2 – magnetic system; 3 – diagnostic ports; 4 – cathode; 5 – insulator; 6 – vacuum-pumping system, A-A and B-B are the cross-sections, where diagnostic ports are located

Table 1

Performance parameters	Typical value
Discharge system: – Discharge voltage, kV – Discharge current, kA – Pulse time, ms – Battery capacity, μF – Stored energy, kJ	 ≤ 5 ≤ 2 ~ 1 560 ≤ 7
Magnetic system: – Voltage, kV – Pulse time, ms – Peak magnetic field, T – Mirror ratio R	 ≤ 3 18 ≤ 0.9 1.25
Vacuum chamber volume, cm^3	~ $7 \cdot 10^4$
Initial pressure, Pa	$1.33 \cdot 10^{-4}$
Operating pressure, Pa	0.133...4.7
Cathode diameter, cm	10
Cathode material	*Ti*
Igniter gas	H_2, Ar, (Kr - Xe - N_2 - O_2)
Plasma volume, cm^3	~ 10^4

2. PARAMETERS FOR DENSE GAS-METAL MULTICOMPONENT PLASMA

Investigations on the formation of dense multicomponent gas-metal plasma in the pulsed reflex discharge were carried out [8 - 16]. The author's scheme [3], employed for introduction of a working metal component, included the following stages: creation of preformed gas plasma using the igniting gas; corpuscular sputtering of a separable cathode material; introduction of the sputtered material into the preformed gas plasma and subsequent ionization. As a result of the investigations, determined were the plasma formation time and plasma lifetime, the maximum density and relative content of the gas and metal components in the plasma, the radial profiles of plasma density and the channels of particle losses at plasma decay. The method of optical emission spectroscopy was used to determine the elemental and charge compositions of the plasma formed in the pulsed reflex discharge. Experimental results testify that the sputtering method, used for working material introduction, is an effective mechanism, providing the formation of plasma with a density of ~ 10^{14} cm^{-3}. It has been established that the highest efficiency of multicomponent gas-metal plasma formation is observed at the electron density $N_e \geq 10^{13}$ cm^{-3}.

Experimentally, it has been found that the plasma layers having different densities are rotating at different angular velocities, and the rotational velocity increases with the magnetic field induction. The radial electric field intensity in the plasma layers of different densities and the plasma particle separation factor have been evaluated. Table 2 lists the plasma parameters for the dense gas-metal multicomponent plasma formed in the reflex discharge.

In addition, a mass increase was observed in the receiving plates placed in the central part of the vacuum (discharge) chamber, along its internal wall. Analysis has shown that the deposit identified on the irradiated plate contains *Ar* and *Ti* being the main components of the gas-metal plasma formed in the reflex discharge under study. Table 3 gives the estimated values of titanium content in the plasma.

Table 2

Parameter	Typical value
Electron density, cm^{-3}	≤ $2 \cdot 10^{14}$
Degree of ionization, %	≤ 100
Density ($N_e = 1 \cdot 10^{13}$ cm^{-3}) formation time, μs: H_2+Ti Ar+Ti (Kr - Xe - N_2 - O_2)+Ti	 ~ 150 ~ 70 ~ 71
Electron temperature, eV	≤ 10…20
Lifetime of plasma density ($N_e \geq 1 \cdot 10^{12}$ cm^{-3}), ms	~ 6…12
Average ion charge	~ 1
Rotational velocity, km/s	0.4…10
Radial electric field, V/cm	≤ 90
Specific flux of Ti sputtering, $mg/cm^2 \cdot s$	~ 0.56

Table 3

Assessment criterion	Titanium content, %
From mass reduction of cathodic substance	30…50 and more
Calculation of plasma density with regard to the processes of sputtering, ionization and diffusion of Ti atoms, $N_e = 2 \cdot 10^{13}$ cm^{-3}, $t = 100$ μs	10…40 and more (depending on the sputtering ratio, ionization rate and diffusion rate)
Measured maximum plasma density, taking into account the density of neutral particles, $t = 180$ μs, $N_e = (1...1.4) \cdot 10^{14}$ cm^{-3}, $Z \sim 1$, $N_0 = 7 \cdot 10^{13}$ cm^{-3}	30…50 and more

3. EFFICIENCY OF IONIZATION PROCESSES OF SPUTTERED ATOMS

First, let us consider the processes associated with the interaction between the plasma and the surface of a solid. These are: sputtering, electron emission induced by the particle-surface interaction; penetration, reflection, and desorption of stimulated particles; modification of the near-surface layer; variations in the charge state of ions; blistering, etc. One of the basic processes leading to the cathode material destruction and, consequently, to its penetration into the plasma, is sputtering. The corresponding major characteristic is the sputtering yield *Y*, which depends on the charge, mass, and energy of bombarding ions; the angle of incidence; the material, of which the target is made; and the target temperature. The sputtering process shows a threshold behavior with respect to the energy.

The sputtering yield and the threshold sputtering energy E_{th} calculated by the model of ref. [18] are depicted in Fig. 2.

In case of the reflex discharge, by virtue of the fact that the plasma rotates, the angle of ion incidence onto the cathode surface can differ considerably from zero. This leads, in turn, to variations in the sputtering yields. The results of corresponding calculations by the model of [19] are shown in Fig. 3.

The specific flux of sputtered substance was determined using the model of [12]. Depending on the sputtering yields (see Fig. 3) at density $N_e = 10^{13}$ cm^{-3} (T_e ~ 8 eV, Ar^+ *E= 1 keV*), the specific flux ranges between ~ 0.24…0.651 mg/cm^2·s ($Ar^+ \rightarrow Ti$), ~ 0.49…1.1 mg/cm^2·s ($Ar^+ \rightarrow Mo$), ~ 0.48…0.94 mg/cm^2·s ($Ar^+ \rightarrow W$), ~ 0.97…1.8 mg/cm^2·s ($Ar^+ \rightarrow U$).

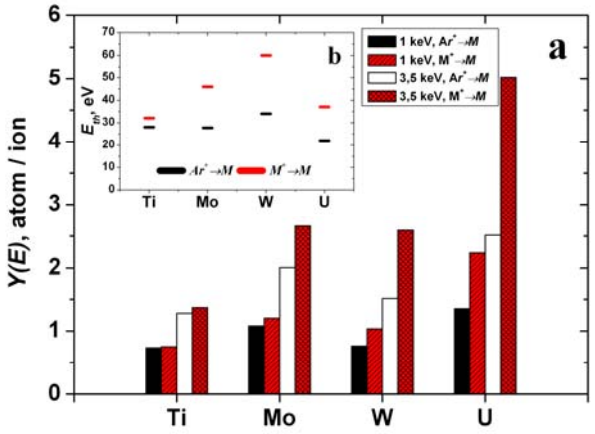

Fig. 2. Sputtering yields of $Ar^+ \rightarrow M$ and self-sputtering $M^+ \rightarrow M$ for different ion energies (normal incidence) (a), sputtering threshold energy (b)

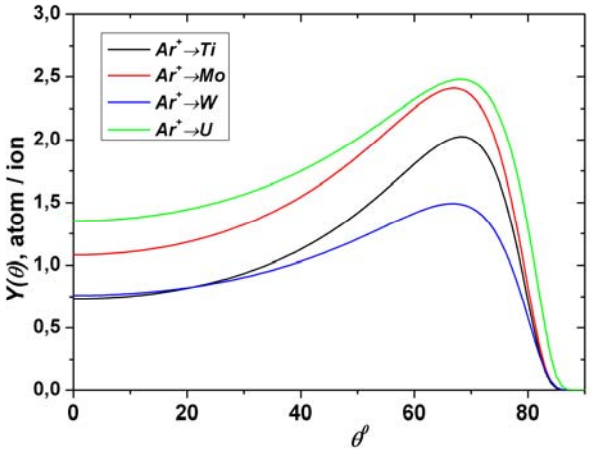

Fig. 3. Sputtering yields versus the angle of ion incidence onto the target material (E= 1 keV)

The efficiencies of the processes of sputtered atom capture into the discharge and gas-metal plasma formation depend on two processes, namely, the diffusion and the ionization of atoms in the primary plasma.

Electron impact ionization is one of the main processes that give rise to the atomic ionization. The following processes can serve as an additional mechanism of ionization for titanium atoms [20]. They are: an ion charge exchange on the atom (the non-resonance charge exchange), ionization at collision with a metastable atom (the Penning process). As was shown in work [21], the Penning ionization dominates over the electron impact ionization in the concentration range below $\leq 2 \cdot 10^{10}$ cm^{-3} and at low temperatures.

In the stationary case where the ionization by electrons is the major ionization process, the balance equations for particles in plasma can be written down in the form:

$$\begin{aligned} \langle \sigma_e v_e \rangle N_e N_M &= \frac{N_{M^+}}{\tau_{M^+}} \\ \langle \sigma_e v_e \rangle N_e N_{Ar} &= \frac{N_{Ar^+}}{\tau_{Ar^+}}, \\ N_e &= N_{Ar^+} + N_{M^+} \end{aligned} \qquad (1)$$

where $\langle \sigma_e v_e \rangle$ is the rate of atom ionization by the electron impact [22, 23]; N_M and N_{Ar} are the concentrations of neutral metal and argon atoms, respectively; N_M^+ and $N_{Ar}^+$are the concentrations of metal and argon ions, respectively; and τ_M^+ and τ_{Ar}^+ are the corresponding lifetimes of ions in plasma. At pressures of interest (<13.33 Pa), the volume recombination of ions is unlikely, and diffusion losses dominate [21]. The ion lifetime is $\tau_{M^+} = \Lambda^2 / D$, where Λ^2 is the characteristic diffusion length, D is the diffusion coefficient [24]. Taking Eq. (1) into account, the degree of ionization can be expressed as:

$$\frac{N_{M^+}}{N_M + N_{M^+}} = \frac{\langle \sigma_e v_e \rangle N_e \tau_{M^+}}{1 + \langle \sigma_e v_e \rangle N_e \tau_{M^+}}. \qquad (2)$$

The results of calculations for the dependences of the degree of metal atom ionization on the electron concentration are presented in Figs. 4 and 5 (the energy distribution function of electrons was assumed to be Maxwellian). For the case of a pulsed discharge (see Fig. 4), where the characteristic times of plasma formation are shorter than the time of ionization equilibration, the degree of ionization strongly depends on the lifetime of plasma with a given electron concentration.

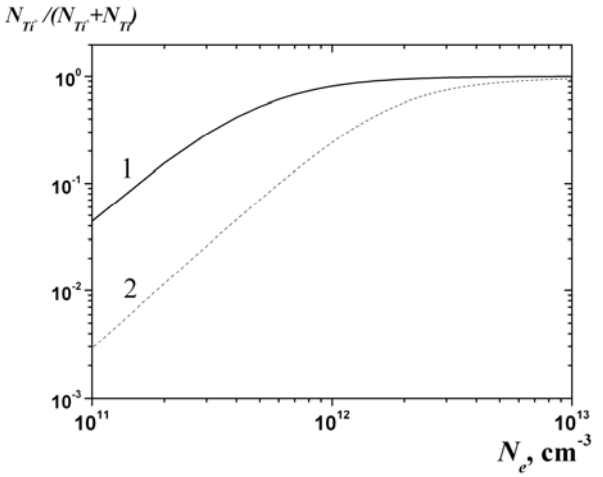

Fig. 4. Degree of titanium atom ionization as a function of the electron concentration (T_e = 8 eV). 1 – steady-state model (present calculation); 2 – time-dependent model [12]

As is seen from Figs. 4 and 5, the efficiency of the gas-metal plasma formation (or, equivalently, the introduction of a working metal substance into the plasma, followed by the metal atom ionization and the gas-metal plasma formation), governed by the mechanism of cathode material sputtering, substantially depends on the initial plasma concentration. The highest efficiency (steady-state model) of the gas-metal plasma generation is observed for the electron concentration $N_e \geq 2 \cdot 10^{12}$ cm^{-3} (see Figs. 4 and 5).

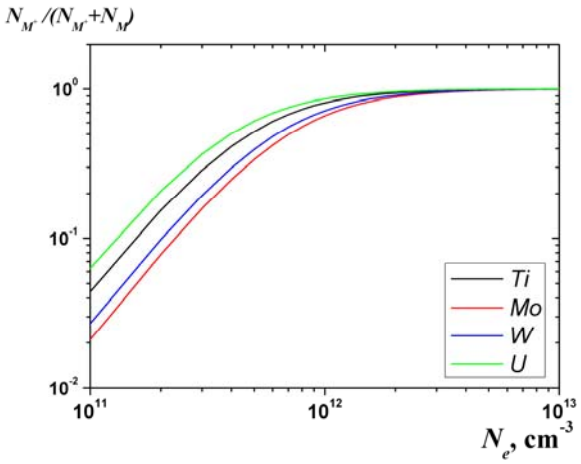

Fig. 5. Degree of metal atom ionization versus electron concentration (T_e = 8 eV)

4. LIMITATION ROTATIONAL VELOCITY OF THE GAS-METAL MULTICOMPONENT PLASMA IN THE REFLEX DISCHARGE

The concept of the critical ionization velocity (CIV) was first introduced by Alfvén [25] as a component of his theory for the formation of the solar system. According to Alfvén hypothesis, a strong interaction leading to efficient ionization will occur when the relative velocity between the plasma and the neutral gas exceeds v_c:

$$v_c = \sqrt{\frac{2 e \phi_i}{m_i}}, \qquad (3)$$

where ϕ_i is the ionization potential and m_i is the mass of the neutral atom or molecule. The first experiment [26] to test the CIV used a homopolar device, in which a neutral gas and a plasma filled the space between two concentric cylinders. The critical velocity (voltage limitation) phenomenon was observed in electrical **E×B** discharges, where the discharge voltage and current were applied across a magnetic field [27 - 29]. Experiments were carried out for the plasma formed in the mono- or two-component gaseous medium. The CIV was observed in the gas-metal plasma formed in high-power impulse magnetron sputtering discharges [30, 31].

A semi-empirical extension of Eq. (3) to binary gas mixtures [32] gives:

$$v_c = \sqrt{\frac{2\left(\alpha e \phi_{i1} + (1-\alpha) e \phi_{i2}\right)}{\alpha m_{i1} + (1-\alpha) m_{i2}}}, \qquad (4)$$

where α is not the mixing ratio, but the fractional rate of component 1 production, i.e., the quantity, which depends on both the mixing ratio and the electron energy.

The results of calculations for the dependences of the critical velocity of binary mixtures on the mixing ratio are presented in Fig. 6.

In the fully ionized case, however, the plasma will interact only with the neutral gas at the end walls and in the boundary regions. The local velocity on a particular field line is then expected to become limited, as soon as it reaches v_c at the end walls. In this case, the isorotation law [1] yields the maximum velocity in the midplane [29] to be:

$$v_{\max} = v_{cr} R^{1/2}, \qquad (5)$$

where R is the mirror ratio. The results of calculations for the dependences of v_{max} on the mirror ratio are presented in Fig. 7.

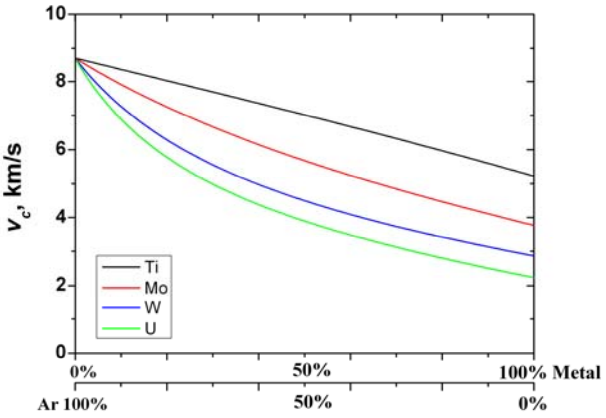

Fig. 6. Critical velocity of binary mixtures versus mixing ratio

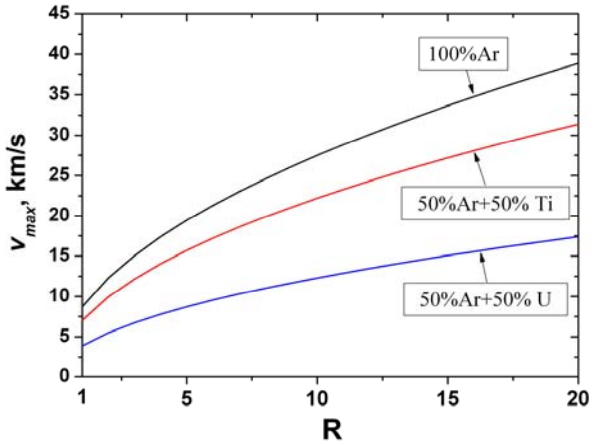

Fig. 7. v_{max} as a function of the mirror ratio

Comparison between the autocorrelation functions of reflected microwave signals, distributed along the magnetic field in the reflex discharge [17], has shown that the periods of these functions are similar, i.e., the angular rotation velocities are close, and this relationship is in accordance with the isorotation law.

At the same time, as it follows from paper [33], the isorotation law may be not always fulfilled in investigations of a laboratory plasma.

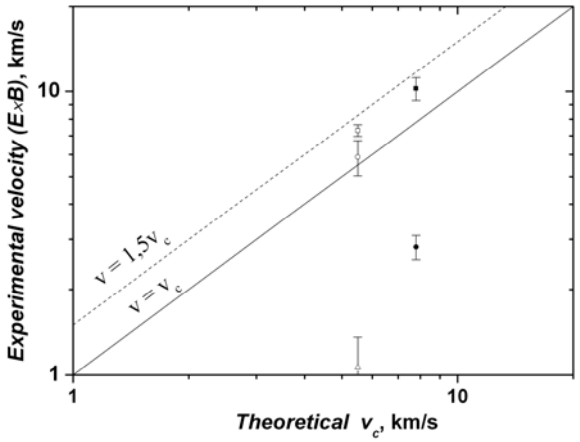

Fig. 8. Comparison between the experimentally observed velocities and the theoretical v_c for the gas-metal plasma

The measured data on the rotational velocity of the gas-metal multicomponent plasma formed in the reflex discharge are presented in Fig. 8. The comparison with theoretical calculations taking into account formulas (4) and (5) shows that the rotational velocity is either lower than the critical velocity or exceeds the CIV by no more than 50%.

In the experiments with all neutral gas-plasma test combinations, made earlier at several different discharge geometries and parameters, the observed rotational velocity was found to hold within typically 50% of Alfven's proposed critical ionization velocity [30], which is what we have in the present experiments (see Fig. 8).

CONCLUSIONS

1. The processes of injection of a sputtered-and-ionized working material into the reflex discharge plasma have been considered at the steady-state model.

2. To determine the efficiency of the gas-metal plasma formation, the following dependences are calculated of the ionization degree of metal particles on the electron concentration. The highest efficiency (steady-state model) of the gas-metal plasma generation is observed for the electron concentration $N_e \geq 2 \cdot 10^{12}$ cm^{-3}.

3. The results of measured rotational velocity of the gas-metal multicomponent plasma formed in the reflex discharge have shown, that rotational velocity is less than critical velocity, or no more than 50% exceeds critical velocity.

REFERENCES

1. B. Lehnert. Rotating plasmas // *Nuclear Fusion*. 1971, v. 11, № 5, p. 485-533.
2. A.J. Fetterman, N.J. Fisch. Metrics for comparing plasma mass filters // *Physics of Plasmas*. 2011, v. 18, № 10, p. 103503 (8 p).
3. Patent of Ukraine 38780, WPC (2006) B01D 59/00. The device for substance separation into elements / E.I. Skibenko, Yu.V. Kovtun, A.I. Skibenko V.B. Yuferov // Appl. 09.07.2008; Publ. 12.01.2009, Bulletin №.1.
4. A.I. Karchevskii, A.I. Lazko, Yu.A. Muromkin, et al. // *Fiz. Plazmy*. 1993, v. 19, № 3, p. 411-419 (in Russian).
5. O.N. Feigenson, Ph.D. thesis (Saint-Petersburg, 2002) (in Russian).
6. E.I. Skibenko, Yu.V. Kovtun, A.M. Yegorov, V.B. Yuferov. Material separation into elements, based on the physical principles of beam-plasma and reflex discharges // *Problems of Atomic Science and Technology. Series «Physics of Radiation Effects and Radiation Materials Science» (97).* 2011, №2(72), p. 141-148.
7. A Compant La Fontaine, P. Louver. Study of an ECR sputtering plasma source // *Plasma Sources Science and Technology*. 1999, v. 8, № 1, p. 125-135.
8. Yu.V. Kovtun, A.I. Skibenko, E.I. Skibenko, et al. Study of the Parameters of Hydrogen–Titanium Plasma in a Pulsed Reflective Discharge // *Plasma Physics Reports*. 2010, v. 36, № 12, p. 1065-1071.
9. Yu.V. Kovtun, A.I. Skibenko, E.I. Skibenko, et al. Study of multicomponent plasma parameters in the pulsed reflex discharge // *Ukrainian Journal of Physics*. 2010, v. 55, № 12, p. 1269-1277.
10. Yu.V. Kovtun, A.I. Skibenko, E.I. Skibenko, et al. Experiment on the production and separation of the pulsed reflective discharge gas-metal plasma // *Technical Physics*. 2011, v. 56, № 5, p. 623-627.
11. Yu.V. Kovtun, E.I. Skibenko, A.I. Skibenko, V.B. Yuferov. Quantitative evaluation of the mass rate of sputtering and separating material in the pulsed reflex discharge // *Problems of Atomic Science and Technology. Series «Vacuum, Pure Materials and Superconductors» (19).* 2011, № 6 (76), p. 85-91.
12. Yu.V. Kovtun, A.I. Skibenko, E.I. Skibenko, V.B. Yuferov. Estimation of efficiency of material injection into the reflex discharge by sputtering the cathode material // *Ukrainian Journal of Physics*. 2012, v. 57, № 9, p. 901-908.
13. Yu.V. Kovtun, A.I. Skibenko, E.I. Skibenko, et al. Influence of the parameters of a pulsed reflex discharge on its plasma characteristics // *Problems of Atomic Science and Technology. Series «Plasma Electronics and New Methods of Acceleration» (7).* 2010, № 4 (68), p. 214-218.
14. Yu.V. Kovtun Dense multicomponent gas-metal reflex-discharge plasma. Ph.D. thesis. Kharkov, 2012, 182 p.
15. Yu.V. Kovtun, A.I. Skibenko, E.I. Skibenko, et al. Radiation of multicomponent gas-metal plasma of a pulsed reflex discharge // *Problems of Atomic Science and Technology. Series «Plasma Physics» (16).* 2010, № 6(70), p. 171-173.
16. Yu.V. Kovtun, A.I. Skibenko, E.I. Skibenko, et al. Determination of the rotational velocity of gas-metal multicomponent plasma in a reflex discharge // *Problems of Atomic Science and Technology. Series «Plasma Physics» (16).* 2010, № 6(70), p. 153-155.
17. Yu.V. Kovtun, A.I. Skibenko, E.I. Skibenko, Propagation of multicomponent plasma oscillations along the magnetic field in the pulsed reflex discharge // *Problems of Atomic Science and Technology. Series «Plasma Physics» (18).* 2012, № 6(82), p. 211-213.
18. Y. Yamamura, H. Tawara. Energy dependence of ion-induced sputtering yields from monoatomic solids at normal incidence // *Atomic Data and Nuclear Data Tables*. 1996, v. 62, p. 149-253.
19. Y. Yamamura. An empirical formula for angular dependence of sputtering yields // *Radiation Effect*. 1984, v. 80, № 1-2, p. 57-72.
20. J.B. Hasted. *Physics of Atomic Collisions.* London: Butterworths. 1964.
21. J. Hopwood, F. Qian. Mechanism for highly ionized magnetron sputtering // *J. Appl. Phys*. 1995, v. 78, № 2, p. 758-765.
22. M.A. Lennon, K.L. Bell, H.B. Gilbody, et al. Recommended Data on the Electron Impact Ionization of Atoms and Ions: Fluorine to Nickel // *Journal of Physical and Chemical Reference Data*. 1988, v. 17, № 3, p. 1285-1363.
23. M.J. Higgins, M.A. Lennon, J. G. Hughes, et al. Atomic and Molecular Data for Fusion, Part 3. Recommended Cross Sections and Rates for Electron Impact Ionization of Atoms and Ions: Copper to

Uranium: Report / Abingdon, 1989. (Prepr. / Culham Laboratory; CLM-R294).
24. B. Bonnevier. Diffusion due to ion-ion collision in a multicomponent plasma // *Arkiv för Fysik*. 1966, v. 33, № 15, p. 255-270.
25. H. Alfvén. On the cosmogony of the solar system // *Stockholms Observatoriums Annaler*. 1942, v. 14, № 2, p. 1-33.
26. H. Alfvén. Collision between a non-ionized gas and a magnetized plasma // *Rev. Mod. Phys.* 1960, v. 32, № 4, p. 710-713.
27. B. Lehnert, J. Bergström, S. Holmberg. Critical voltage of a rotating plasma // *Nuclear Fusion*. 1966, v. 6, № 3, p. 231-238.
28. C. Teodorescu, R. Clary, R.F. Ellis, et al. Experimental study on the velocity limits of magnetized rotating plasmas // *Physics of Plasmas*. 2008, v. 15, № 4, p. 042504.
29. I.C. Teodorescu, R. Clary, R.F. Ellis, et al. Sub-Alfvenic velocity limits in magnetohydrodynamic rotating plasmas // *Physics of Plasmas*. 2010, v. 17, № 5, p. 052503 (13 p).
30. N. Brenning, D. Lundin. Alfvén's critical ionization velocity observed in high-power impulse magnetron sputtering discharges // *Physics of Plasmas*. 2012, v. 19, № 9, p. 093505.
31. N. Brenning, D Lundin, T Minea, et al. Spokes and charged particle transport in HiPIMS magnetrons // *J. Phys. D: Appl. Phys.* 2013, v. 46, № 8, p. 084005 (10 p).
32. I. Axnas. Experimental investigation of the critical ionization velocity in gas mixtures // *Astrophysics and Space Science*. 1978, v. 55, № 1, p. 139-146.
33. C.A. Romero-Talamás, R.C. Elton, W.C. Young, et al. Isorotation and differential rotation in a magnetic mirror with imposed E×B rotation // *Physics of Plasmas*. 2012, v. 19, № 7, p. 072501.

Article received 12.04.2013.

ОСОБЕННОСТИ ОБРАЗОВАНИЯ ПЛОТНОЙ ПЛАЗМЫ ОТРАЖАТЕЛЬНОГО РАЗРЯДА НА ГАЗОМЕТАЛЛИЧЕСКИХ СМЕСЯХ

Ю.В. Ковтун

Кратко суммированы авторские данные по исследованию многокомпонентной газометаллической плазмы импульсного отражательного разряда. Проведено рассмотрение процессов ввода рабочего вещества (Ti, Mo, W, U) за счет распылительного механизма и его ионизации в плазме отражательного разряда для стационарной модели. Результаты измерения скорости вращения газометаллической многокомпонентной плазмы, образованной в отраженном разряде, коррелируют с критической скоростью ионизации, CIV.

ОСОБЛИВОСТІ УТВОРЕННЯ ГУСТОЇ ПЛАЗМИ ВІДБИВНОГО РОЗРЯДУ У ГАЗОМЕТАЛЕВИХ СУМІШКАХ

Ю.В. Ковтун

Стисло підсумовані авторські дані по дослідженню багатокомпонентної газометалевої плазми імпульсного відбивного розряду. Розглянуто процеси, пов'язані з введенням робочої речовини (Ti, Mo, W, U) у плазму відбивного розряду за рахунок розпилюючого механізму для стаціонарної моделі. Результати вимірювання швидкості обертання газометалевої багатокомпонентної плазми, утвореною у відбитому розряді, корелюють з критичною швидкістю іонізації, CIV.